

Robust superconductivity and fragile magnetism induced by the strong Cu impurity scattering in the high-pressure phase of FeSe

Z. Zajicek,^{1,*} S. J. Singh,¹ and A. I. Coldea^{1,†}

¹Clarendon Laboratory, Department of Physics, University of Oxford, Parks Road, Oxford OX1 3PU, UK

(Dated: December 13, 2022)

Superconductivity in FeSe is strongly enhanced under applied pressure and it is proposed to emerge from anomalously coupled structural and magnetic phases. Small impurities inside the Fe plane can strongly disrupt the pair formation in FeSe at ambient pressure and can also reveal the interplay between normal and superconducting phases. Here, we investigate how an impurity inside the Fe plane induced by the Cu substitution can alter the balance between competing electronic phases of FeSe at high pressures. In the absence of an applied magnetic field, at low pressures the nematic and superconducting phases are suppressed by a similar factor. On the other hand, at high pressures, above 10 kbar, the superconductivity remains unaltered despite the lack of any signature in transport associated to a magnetic phase in zero-magnetic field. However, by applying a magnetic field, the resistivity displays an anomaly preceding the activated behaviour in temperature, assigned to a magnetic anomaly. We find that the high-pressure superconducting phase of FeSe is robust and remains enhanced in the presence of Cu impurity, whereas the magnetic phase is not. This could suggest that high- T_c superconductivity has a sign-preserving order parameter in a presence of a rather glassy magnetic phase.

Introduction. Hydrostatic pressure is an invaluable tool to stabilize novel electronic phases as well as to enhance superconductivity towards room temperature [1]. Among unconventional superconductors, FeSe displays the signature of a nematic electronic phase before becoming superconducting at low temperatures below 9 K [2]. However, with applied pressure the nematic phase is suppressed and the superconducting transition temperature is enhanced towards 37 K close to 6.3 GPa [3–9]. This enhanced superconductivity at high pressures occurs in a region in which a new electronic phase, believed to be of magnetic origin (spin-density wave (SDW) phase), is present [10, 11]. The volume and the local magnetic field of this magnetic phase is strongly dependent on the applied pressure [10] and it coincides with a first-order structural transition at high pressures, suggesting a potential magnetoelastic coupling and phase coexistence [11]. Interestingly, this magnetic phase follows the superconducting phase very closely at high pressures, and it raises the question whether bulk superconductivity coexists or competes on short-length scales with the magnetic order [10]. Furthermore, the enhancement of superconductivity is also present in $\text{FeSe}_{1-x}\text{S}_x$ under pressure, even though the signatures associated with any magnetic order are strongly reduced with increased iso-electronic substitution [12].

Another tuning parameter of superconducting and nematic phases of FeSe is the chemical substitution either inside or outside the conducting Fe plane. The Cu substitution is highly disruptive, due to the larger size of the Cu relative to the Fe ions inside the conducting planes, which introduces significant impurity scattering. The nematic and superconducting phases are suppressed linearly up to 3% Cu substitution, whereas the carrier mobilities are quickly reduced even with a small amount of Cu substitution [13–15]. By increasing the Cu substitution the system undergoes a metal-to-insulator transition which could lead to the stabilization of local magnetic moments at Fe sites [15–17]. However, under applied hydrostatic pressure the superconductivity of $\text{Fe}_{1-x}\text{Cu}_x\text{Se}$

could be restored by suppressing the insulating behaviour in powder samples [18] or by quenching from high pressures in single crystals [19]. These reports highlight that the high-pressure superconductivity stabilized under pressure is robust while signatures of any magnetic order are not detected. Theoretical studies suggest that non-magnetic disorder can have the potential to enhance superconductivity in a multi-band system [20], and thus the Cu substitution can be used to assess this proposal and to understand its unusual manifestation.

In this paper, we report a transport study of the effect of a small amount of Cu substitution ($x \sim 0.0025$) in FeSe under applied hydrostatic pressure up to 20 kbar to understand the response of the superconducting, nematic and magnetic phases. Despite the suppression of the nematic and superconducting phases at low pressures compared to FeSe, the high pressure superconducting phase is robust against the Cu substitution. In the absence of an applied magnetic field, we observe no anomaly in resistivity, often associated to a SDW phase in FeSe, but a broad superconducting transition invoking that the electronic conduction at high pressures above 10 kbar is still affected by the Cu substitution. However, in strong magnetic fields we detect an upturn in resistivity which is strongly hysteretic suggestive of glassy behaviour. Furthermore, we detect a reduction of the charge carrier mobilities and increased scattering rate with increasing pressure, in this region remains with robust superconductivity.

Methods. Single crystals of $\text{Fe}_{1-x}\text{Cu}_x\text{Se}$, with the nominal composition of $x = 0.0025(4)$ were grown using the KCl/AlCl₃ chemical vapour transport method [21, 22], as reported previously in [14]. Magnetotransport studies under pressure were carried out in a 16 T Quantum Design PPMS. The in-plane resistivity ρ_{xx} and Hall ρ_{xy} components were measured using a low-frequency five-probe technique and were separated by (anti)symmetrizing data measured in positive and negative magnetic fields with the magnetic field applied along the c -axis ($I \parallel (ab)$). Good electrical contacts were achieved by In soldering and currents up to 1 mA (peak-to-

peak) were used to avoid heating. The pressure studies were performed using a piston-cylinder cell and Daphne Oil 7373 up to 21 kbar. The pressure at low temperatures was determined via the superconducting transition temperature of Sn after cancelling the remnant magnetic field [23]. Errors in the exact contact positions and size result in errors of up to 13% of absolute values of resistivity. The superconducting transitions, T_c and H_{c2} , are defined as the offset temperature or field, respectively, unless stated otherwise. The nematic structural transition, T_s , and the high pressure magnetic phase transition, T_m , are defined by the minimum in the derivative of the resistivity as a function of temperature, as in previous studies [24].

Transport studies under applied pressure. Fig. 1(a) shows the temperature dependence of the resistivity in the absence of a magnetic field for pressures up to 20 kbar (see shifted curves in Fig. S1 in the Supplemental Material (SM) [25]). Due to the presence of Cu, the nematic transition T_s , at 80 K, and superconducting transition, T_c , at 6.2 K are suppressed, as compared with FeSe [14]. Under applied pressure, the nematic transition is linearly suppressed with applied pressure up to 15 kbar, similar to FeSe [26], whereas the superconductivity is continuously enhanced with applied pressure up to 20 kbar, without showing any dome like-feature visible for FeSe [26]. The superconducting transition width, ΔT_c , is around 1.3(2) K, before increasing by a factor of 2 at higher pressures above 10 kbar, as shown in Fig. 1(b). In FeSe under pressure the superconducting transition width is sharp (< 1 K) at low pressures before increasing significantly towards 7 K for pressures where the magnetic phase is present [24]. This suggests that either the high pressure superconducting phase becomes inhomogeneous in the presence of another competing phase, or that strong superconducting and/or magnetic fluctuations are present in this high pressure regime [26].

The resistivity behaviour provides additional information about the normal electronic phases as a function of pressure. At room temperature, the resistivity initially decreases with increasing pressure, indicating that the in-plane transfer integrals are larger under pressure which increases the bandwidth and the system becomes a better metal, as shown in Fig. 1(b). However, at higher pressures above 15 kbar this trend reverses with resistivity increasing again, also observed at low temperatures (see Fig. S1(b) in the SM [25]). The substitution of Cu in FeSe increases the impurity scattering and the residual resistivity, leading to the suppression of superconductivity and inducing a linear dependence down to 0.4 K [14]. Under pressure, the linear dependence is found both inside the nematic phase at low pressures as well as in the high pressure phase, as also illustrated by the temperature dependence of the resistivity exponent, n in Figs. S1(c) and (d) in the SM [25]. At high temperatures in the tetragonal phase, the resistivity can be described by a power law of $T^{1.5}$ which is rather similar to that observed for both $\text{FeSe}_{1-x}\text{S}_x$, tuned either by the isoelectronic substitution or applied pressure [27, 28]. Interestingly, in the high pressure regime above 10 kbar the resistivity of Cu-substituted FeSe shows no additional anomaly associated to

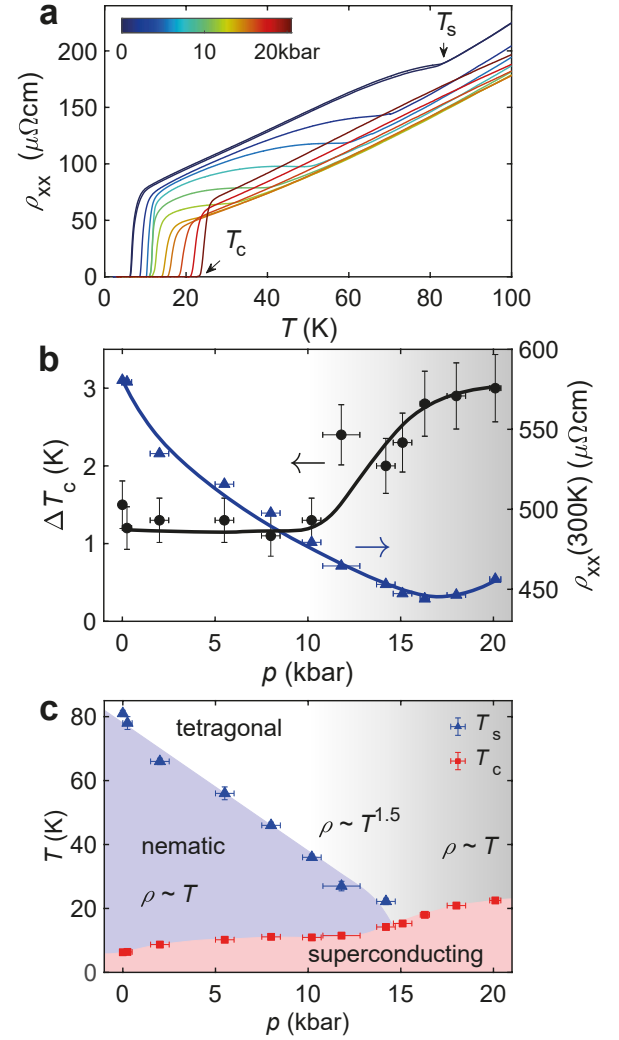


FIG. 1. Zero-field transport properties of $\text{Fe}_{1-x}\text{Cu}_x\text{Se}$ under pressure. (a) Temperature dependence of the resistivity as a function of applied pressure. (b) The evolution of the superconducting transition width, $\Delta T_c = T_{\text{on}} - T_{\text{off}}$ (black circles), and the resistivity at 300 K (blue triangles) with pressure. Solid lines are guides to the eye. (c) Temperature-pressure phase diagram in zero magnetic field tuned by pressure. The nematic phase occurs at T_s (blue triangles) and superconductivity has the offset temperature at T_c (red squares). The phase diagram can be divided into three different regions: the low pressure region up to $p_1 = 10$ kbar, inside the nematic phase, the high-pressure region above $p_2 = 15$ kbar, once the nematic phase is fully suppressed, and the intermediate pressure region between p_1 and p_2 . The shaded areas indicate different phase boundaries.

other phase transitions (see Figs. 1(a) and S1 in the SM [25]). This is in contrast to FeSe where a clear upturn in the resistivity anomalies was associated with the presence of a magnetic transition at a temperature above T_c [9, 24, 26, 29].

Based on these transport studies, the zero-field temperature-pressure phase diagram of the $\text{Fe}_{1-x}\text{Cu}_x\text{Se}$ up to 20 kbar is constructed, as shown in Fig. 1(c). At high pressures, the superconducting transition temperature, T_c , increases once the nematicity is suppressed even in the presence of the Cu impu-

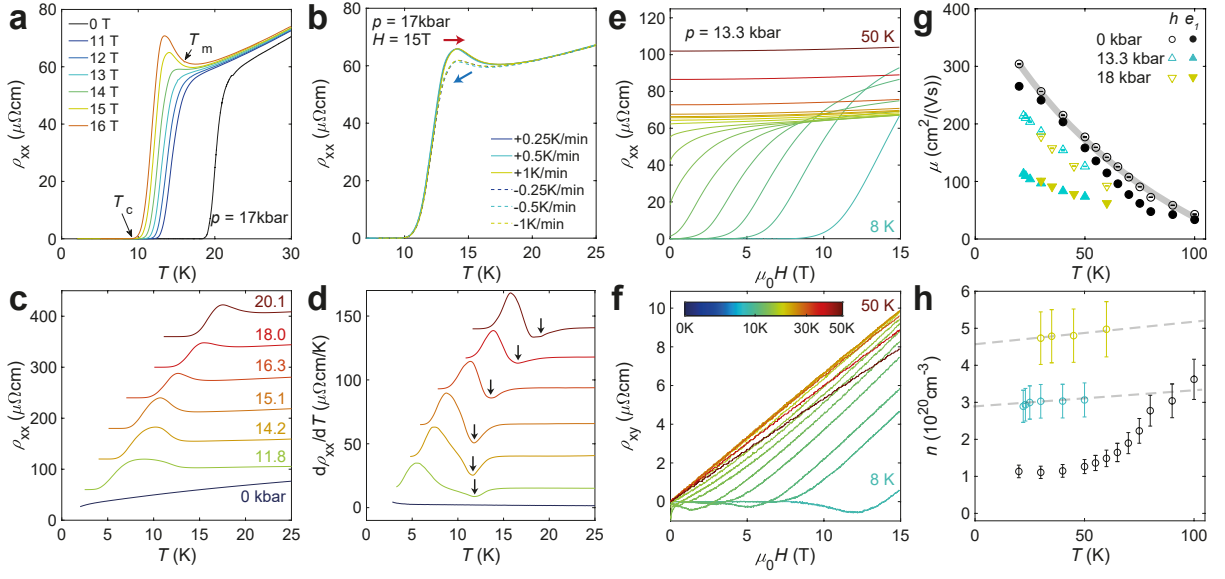


FIG. 2. **The transport behaviour in magnetic field of the $\text{Fe}_{1-x}\text{Cu}_x\text{Se}$ under pressure.** (a) The temperature dependence of the longitudinal resistivity in different magnetic fields at $p = 17$ kbar. (b) The resistivity upturn at T_m in 15 T at 17 kbar using various temperature sweep rates. The solid lines correspond to the warming sweeps whereas the dashed lines correspond to the cooling sweeps. (c) The temperature dependence of resistivity in a magnetic field of 15 T ($H||c$) for different applied pressures and (d) their corresponding derivatives. The value of T_m is defined as the minimum in the derivative and indicated by arrows, similar to FeSe [12]. Curves are offset for clarity. Field dependence of (e) the longitudinal resistivity, ρ_{xx} , and (f) the Hall resistivity, ρ_{xy} , at a pressure of $p = 13.3$ kbar. (g) Mobility and (h) carrier density of each charge carrier (hole, h and electron e_1) considering a two-band compensated model ($n_h = n_{e_1}$) at different pressures. The two-band model at ambient pressure uses data below < 7 T and a three-band could be used to describe the full field window, as reported in Ref. [14] and shown in Fig. S7 in the SM. Solid and dashed lines are guides to the eye.

ity. This behaviour is in agreement with previous studies in powder samples of Cu substituted FeSe, where an insulating phase is transformed into a superconductor with applied pressure, although not to a zero resistance state [18]. Furthermore, the phase diagram in zero-magnetic field in the presence of the Cu impurity inside the conducting plane is remarkably similar to that of $\text{FeSe}_{1-x}\text{S}_x$, in which the isoelectronic substitution takes place outside the conducting plane [12, 28, 30, 31].

The high-pressure electronic phase in high magnetic fields. Next, we use high magnetic fields to suppress the superconductivity to reveal any hidden electronic phases and to explore the normal electronic behaviour at lower temperatures, once the superconductivity is suppressed. Fig. 2(a) shows the temperature dependence of resistivity in different magnetic fields at 17 kbar, in which an upturn occurs at T_m , as the temperature is reduced in large enough magnetic field. This anomaly shows hysteretic behaviour between the cooling and warming curves, independent of the temperature sweep rate, indicative of a first-order phase transition, as shown in Fig. 2(b). In FeSe, the high pressure magnetic phase displays evidence of hysteresis in heat capacity and NMR studies, implying the existence of a concomitant structural transition via a spin-lattice coupling [26, 32]. The temperature dependence of the resistivity in 15 T shows smooth changes in the upturn anomaly as a function of the applied pressure, as shown in Fig. 2(c) and the corresponding derivatives in Fig. 2(d). As the pressure increases, this anomaly shifts to higher temperatures and

it tracks closely the zero field superconducting transition temperature. In FeSe, this anomaly was associated to a magnetic phase and it occurs already in zero-field at a higher transition temperature than the superconducting transition, T_c , but its appearance seems to vary strongly with pressure, either as an increase, decrease or change in slope [9].

Magnetotransport behaviour. The magnetotransport studies can provide valuable insight into the changes in the electronic structure and scattering with applied pressure. Figs. 2(e) and (f) show the field dependence of the longitudinal and Hall resistivity, ρ_{xx} and ρ_{xy} , at 13.3 kbar. The presence of the linear field-dependence of the Hall component indicates a two-band behaviour which describe the behaviour inside the high pressure and the tetragonal phase (see Figs. S3, S4, and S5 in the SM [25]). At high pressures, the Hall coefficient extracted from the slope of the Hall resistivity in low fields, ρ_{xy} , is positive and generally increases with decreasing temperature, as shown in Fig. S7(f) in the SM [25]. This is in stark contrast to FeSe which displays negative Hall coefficient at low temperatures inside the nematic phase both at ambient and at low pressures [33–35].

Magnetotransport measurements enable the extraction of the charge carrier density and mobilities by simultaneously fitting the ρ_{xx} and ρ_{xy} components to a two-band compensated model. We use the initial input parameters from the mobility spectrum, whose peaks indicate that the mobilities are slightly reduced with increasing pressure (see Fig. S6 in the SM [25]).

In order to compare the parameters between different pressure regions, we use a two-band compensated model in low-field regime (< 7 T) for ambient pressure rather than the three-band compensated model which can account for the non-linear Hall resistivity, similar to FeSe [14, 34, 36]. Figs. 2(g) and (h) compare the temperature dependence of the charge carrier mobilities and carrier densities at various pressures (see also Fig. S7 in the SM [25]). Upon entering the nematic phase from high temperatures there is a significant decrease in the apparent carrier density, n , due to the development of anisotropic scattering, as found for FeSe [34, 36]. In the high pressure phase, the carrier density is significantly larger indicative of an increase of the Fermi surface size similar to findings for $\text{FeSe}_{1-x}\text{S}_x$ [28]. Furthermore, the mobilities of both holes and electrons are suppressed with applied pressure, with stronger suppression for the negative charge carriers, similar to findings in thin flakes of FeSe [34]. This could indicate an increased scattering rate of spin fluctuations at high pressures and/or an increase in effective mass, which is consistent with the enhanced resistivity found in the high pressure phase of Cu-substituted FeSe shown in Fig. 1(b). This behaviour is rather similar to that of FeSe under pressure, where a three-band model is required to explain its low temperature behaviour for all pressures, but the carrier densities are enhanced and the mobilities decreased with increasing pressure [37].

The pressure-temperature p - T phase diagrams. To summarize we compare the temperature-pressure phase diagram of Cu-FeSe with that of FeSe [24] in 0 T and 15 T, as shown in Figs. 3(a) and (b). The phase diagram can be split into three distinct regions: firstly, in the low pressure region, $p < p_1 \sim 10$ kbar, the superconducting phase emerges from the nematic phase, secondly at intermediate pressures, $p_1 < p < p_2 \sim 15$ kbar, signatures of the magnetic phase are detected in FeSe in zero-field and finally, at higher pressures, $p > p_2$ the magnetic and superconducting phases coexist and the nematic phase is suppressed at p_2 . Interestingly, as the pressure increases beyond p_1 , T_c displays a broadly similar pressure dependence for the two systems, indicating a robustness of superconductivity to impurity scattering. The increase in T_c occurs in a regime where the carrier density n increases at high pressure, as shown in Fig. 2(h). On the other hand, the magnetic phase above p_2 is highly sensitive to impurity scattering, being washed out by the small amount of the Cu substitution and its signatures are only visible in magnetic field, as shown in Fig. 3(b). The upper critical field across these phases shows a remarkable scaling to T_c in the presence of the Cu impurity across the phase diagram (Fig. S7 in the SM).

In order to account for the relative changes in superconductivity due to the Cu substitution, the temperature-pressure diagrams are scaled to their ambient value of T_s , as shown in Fig. 3(c). We notice a remarkable scaling of the nematic and superconducting temperatures between FeSe and Cu-FeSe, up to p_1 , suggesting that the impurity scattering affects the two phases in a similar manner and have a similar origin, as found also for higher Cu substitution [13, 14]. As the superconductivity at low pressure is strongly suppressed by the Cu substi-

tution, this is consistent with sign-changing s_{\pm} -type of order parameter in the low pressure regime [14].

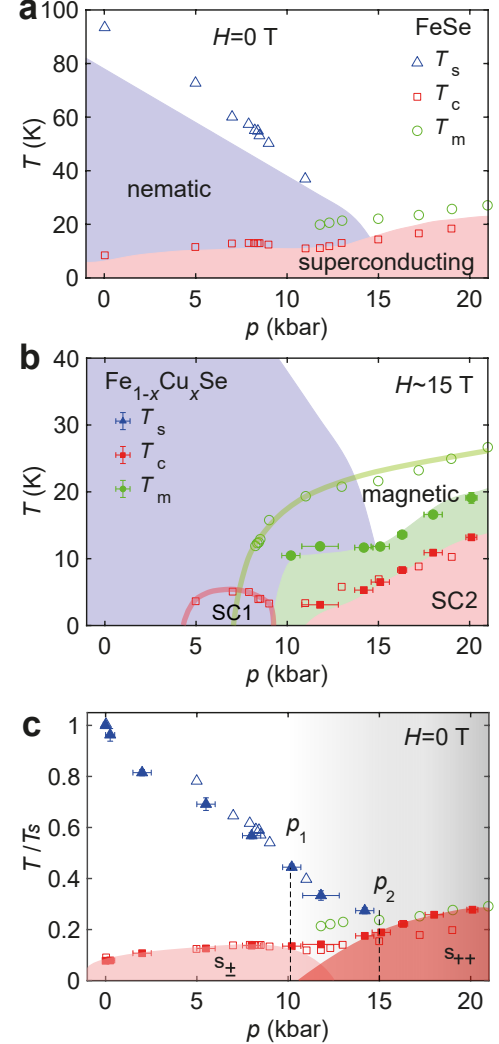


FIG. 3. The pressure-temperature phase diagrams of Cu substituted FeSe. The comparison between the different electronic phases of FeSe (open symbols) from Ref. 24 and Cu-FeSe (solid symbols) measured in (a) 0 T and (b) in 15 T for Cu-FeSe and 16 T for FeSe (after Ref. [24]). The shaded areas in all panels reflect the phase boundaries for Cu-FeSe, as described in Fig. 1(c). The solid lines in (b) are guides to the eye for FeSe. Nematic shaded area in (a) and (b) are for Cu-FeSe, assuming a field-independent T_s . (c) The scaling of the temperature-pressure phase diagram from (a) by using the reduced temperature $t = T/T_s$, where T_s is the nematic transition at ambient pressure for the two systems. The two shaded regions reflect schematically the two proposed superconducting regions with the boundaries given by the maximum value of T_c .

Interestingly, at high pressure above p_2 the magnetic and superconducting phases of FeSe enhance their transition temperatures with increasing pressure [26]. However, the very small Cu substitution is sufficient to break down this trend and only superconductivity is present, whereas the signatures of the magnetic phase in resistivity have disappeared. This sug-

gest the fragility of the magnetic phase which is only detected and stabilized by the presence of a magnetic field. In high magnetic fields (~ 15 T), the magnetic transition is strongly suppressed in the Cu-FeSe as compared with FeSe, whereas the superconducting domes are rather similar, as shown in Fig. 3(b). This suggests that the superconducting phase at high pressure is robust in the presence of the Cu impurity.

Significant disruption of the high pressure magnetic phase was also detected under pressure in FeSe crystals with higher disorder [38, 39], as well as in thin flakes of FeSe under pressure, where the magnetic phase is suppressed as the thickness decreases [40]. Interestingly, in the presence of sulphur substitution outside the Fe planes, the magnetic phase is also suppressed at lower pressures in $\text{FeSe}_{1-x}\text{S}_x$, although it was suggested to be stabilized at higher pressures around 50 kbar [12]. The robust superconductivity at high pressure occurs up to 31 K also in the presence of large amount of the Cu substitution towards 4% but there are no signatures of a magnetic phase [18, 38, 39]. This implies that the superconductivity in the high pressure phase of FeSe and Cu-FeSe is rather robust to impurity scattering, which would be consistent with an s_{++} pairing symmetry or that the high-pressure superconductivity is strongly inhomogeneous. In the latter case, the superconducting order could still have a s_{\pm} pairing symmetry since extended emergent disorder regions are unable to provide large-momentum transfer interband scattering connecting opposite signs of the superconducting gap function on electron and hole pockets, and therefore strongly limiting any substantial pair-breaking processes from the inhomogeneous disorder landscape. However, for superconductors with a sign-reversal order parameter the T_c is strongly suppressed by impurity scattering, as found for the Cu-substituted FeSe inside the nematic phase [14]. Theoretically, it is suggested that disorder in multi-band superconductors can cause a transition between s_{+-} and s_{++} pairing symmetry if one of two gaps changes sign and T_c is predicted to remain finite and almost independent of the impurity scattering rate [41]. Additionally, superconductivity could be enhanced for a sign-preserving gap, even in the presence of large enough disorder, as disorder can induce spatial modulations where the coherence length is a few nanometers [20, 42]. Fig. 3(c) indicates the separation into two superconducting domes of potentially different symmetry and response to impurity scattering of the $p-T$ phase diagram of Cu-FeSe. Interestingly, two superconducting domes are also present for $\text{FeSe}_{0.89}\text{S}_{0.11}$, in which the isoelectronic substitution occurs outside the conducting plane, and no signature of a magnetic phase is detected at the high-pressure phase up to 22 kbar [28].

The enhanced resistivity at high pressures, combined with the reduction of mobilities while the apparent carrier density increases, imply that either the high-pressure phase is highly inhomogeneous or that there are very strong spin fluctuations that do not permit the stabilization of the long-range magnetic order. These effects are also evident in the evolution of the superconducting transition width which becomes extremely broad above p_1 both in FeSe and Cu-FeSe, as shown

in Fig. 1b. The large hysteresis effects observed in the resistivity curves for different cooling rates in the high pressure phase suggest that the local short-range magnetic order is affected by the presence of Cu ions, by freezing of dynamical spin fluctuations of the Fe magnetic moments in the presence of non-magnetic disorder [43]. Evidence of short-range local magnetism was found in FeSe under pressure using μSR as well as Mossbauer spectroscopy [10, 11], but neutron diffraction studies have not been able to resolve any long-range magnetic order [44].

Theoretical calculations of non-magnetic impurities in FeSe show that point-like disorder sites locally induce short-range magnetism [45, 46]. The presence of the Cu impurity inside the SDW phase can lead to phase fragmentation or glassy behaviour, similar to a SDW glass proposed to arise in systems with weak non-magnetic disorder [47]. Microscopic calculations inside the SDW phase of iron-based superconductors have suggested that a strong non-magnetic potential, like Cu, can generate extended magnetic nematogens, which are regions of a competing magnetic phase centered at the impurity site (typical lengths of ~ 10 lattice constants) [46]. Such entities could be short-circuited in transport studies at high pressure leading to the vanishing of the SDW signatures, despite the tiny amount of Cu in the samples. An external field, however, could potentially re-align and couple the induced magnetic puddles and thereby introduce additional spin-dependent scattering which can enhance resistivity and mimic the behaviour in the absence of the Cu impurities. Spatially-resolved probes would be very valuable for obtaining a detailed understanding of the fascinating interplay between disorder, magnetism and superconductivity in the high-pressure region of FeSe. Theoretical work addressing the nature and the robustness of the high-pressure superconducting phase, specific to FeSe and its related systems, would be very valuable to guide experimental findings and to help identify the essential ingredients to design a high-temperature superconductor.

Conclusions Our study provides new insight into the nature of unconventional superconductivity of FeSe in different regimes and its sensitivity to impurity scattering in the presence of a small amount of Cu substitution. The magnetic phase at high pressures is profoundly affected by the impurity scattering that can lead to a phase separation between the superconducting and magnetic phases with a hysteretic first-order transition. At low pressures, nematic and superconducting phases are suppressed by the Cu impurity, consistent with the presence of a sign-changing pairing. On the other hand, the robustness of the high-pressure superconducting phase, despite the fragility of the magnetic phase, implies either a non-sign changing superconducting phase, or a highly inhomogeneous phase with mainly extended scattering regions with suppressed pair-breaking effects for s_{\pm} superconductivity. Further theoretical work is required to understand how to stabilize such a robust superconductivity, in the absence of applied pressure.

Acknowledgements We thank Brian Andersen, Peter Hirschfeld, Maria Gastiasoro, and Pascal Reiss for very useful discussions and comments on the manuscript. This work was mainly supported by EPSRC (EP/I004475/1) and Oxford Centre for Applied Superconductivity. We also acknowledge financial support of the John Fell Fund of the Oxford University. Z.Z. acknowledges financial support from the EPSRC studentship (EP/N509711/1). AIC acknowledges an EPSRC Career Acceleration Fellowship (EP/I004475/1).

* corresponding author: zachary.zajicek@physics.ox.ac.uk

† corresponding author: amalia.coldea@physics.ox.ac.uk

- [1] E. Snider, N. Dasenbrock-Gammon, R. McBride, M. Debessai, H. Vindana, K. Vencatasamy, K. V. Lawler, A. Salamat, and R. P. Dias, Room-temperature superconductivity in a carbonaceous sulfur hydride, *Nature* **586**, 373 (2020).
- [2] A. I. Coldea and M. D. Watson, The key ingredients of the electronic structure of FeSe, *Annu. Rev. Cond. Matt. Phys.* **9**, 10.1146/annurev-conmatphys-033117-054137 (2018).
- [3] Y. Mizuguchi, F. Tomioka, S. Tsuda, T. Yamaguchi, and Y. Takano, Superconductivity at 27K in tetragonal FeSe under high pressure, *Applied Physics Letters* **93**, 152505 (2008), <https://doi.org/10.1063/1.3000616>.
- [4] S. Medvedev, T. M. McQueen, I. A. Troyan, T. Palasyuk, M. I. Erements, R. J. Cava, S. Naghavi, F. Casper, V. Ksenofontov, G. Wortmann, and C. Felser, Electronic and magnetic phase diagram of β -Fe_{1.01}Se with superconductivity at 36.7 K under pressure, *Nat. Mater.* **8**, 630 (2009).
- [5] G. Garbarino, A. Sow, P. Lejay, A. Sulpice, P. Toulemonde, M. Mezouar, and M. Núñez-Regueiro, High-temperature superconductivity (T_c onset at 34 K) in the high-pressure orthorhombic phase of FeSe, *EPL (Europhysics Letters)* **86**, 27001 (2009).
- [6] D. Braithwaite, B. Salce, G. Lapertot, F. Bourdarot, C. Marin, D. Aoki, and M. Hanfland, Superconducting and normal phases of FeSe single crystals at high pressure, *Journal of Physics: Condensed Matter* **21**, 232202 (2009).
- [7] S. Margadonna, Y. Takabayashi, Y. Ohishi, Y. Mizuguchi, Y. Takano, T. Kagayama, T. Nakagawa, M. Takata, and K. Prasad, Pressure evolution of the low-temperature crystal structure and bonding of the superconductor FeSe ($T_c = 37$ K), *Phys. Rev. B* **80**, 064506 (2009).
- [8] S. Masaki, H. Kotegawa, Y. Hara, H. Tou, K. Murata, Y. Mizuguchi, and Y. Takano, Precise Pressure Dependence of the Superconducting Transition Temperature of FeSe: Resistivity and ⁷⁷Se-NMR Study, *Journal of the Physical Society of Japan* **78**, 063704 (2009), <https://doi.org/10.1143/JPSJ.78.063704>.
- [9] J. P. Sun, K. Matsuura, G. Z. Ye, Y. Mizukami, M. Shimozawa, K. Matsubayashi, M. Yamashita, T. Watashige, S. Kasahara, Y. Matsuda, J.-Q. Yan, B. C. Sales, Y. Uwatoko, J.-G. Cheng, and T. Shibauchi, Dome-shaped magnetic order competing with high-temperature superconductivity at high pressures in FeSe, *Nat. Commun.* **7**, 12146 (2016).
- [10] M. Bendele, A. Amato, K. Conder, M. Elender, H. Keller, H.-H. Klauss, H. Luetkens, E. Pomjakushina, A. Raselli, and R. Khasanov, Pressure Induced Static Magnetic Order in Superconducting FeSe_{1-x}, *Phys. Rev. Lett.* **104**, 087003 (2010).
- [11] A. E. Böhmer, K. Kothapalli, W. T. Jayasekara, J. M. Wilde, B. Li, A. Sapkota, B. G. Ueland, P. Das, Y. Xiao, W. Bi, J. Zhao, E. E. Alp, S. L. Bud'ko, P. C. Canfield, A. I. Goldman, and A. Kreyssig, Distinct pressure evolution of coupled nematic and magnetic orders in FeSe, *Phys. Rev. B* **100**, 064515 (2019).
- [12] K. Matsuura, Y. Mizukami, Y. Arai, Y. Sugimura, N. Maejima, A. Machida, T. Watanuki, T. Fukuda, T. Yajima, Z. Hiroi, K. Y. Yip, Y. C. Chan, Q. Niu, S. Hosoi, K. Ishida, K. Mukasa, S. Kasahara, J.-G. Cheng, S. K. Goh, Y. Matsuda, Y. Uwatoko, and T. Shibauchi, Maximizing T_c by tuning nematicity and magnetism in FeSe_{1-x}S_x superconductors, *Nat. Comm.* **8**, 1143 (2017).
- [13] C. Gong, S. Sun, S. Wang, and H. Lei, Normal and superconducting state properties of Cu-doped FeSe single crystals, *Phys. Rev. B* **103**, 174510 (2021).
- [14] Z. Zajicek, S. J. Singh, H. Jones, P. Reiss, M. Bristow, A. Martin, A. Gower, A. McCollam, and A. I. Coldea, Drastic effect of impurity scattering on the electronic and superconducting properties of Cu-doped FeSe, *Phys. Rev. B* **105**, 115130 (2022).
- [15] A. J. Williams, T. M. McQueen, V. Ksenofontov, C. Felser, and R. J. Cava, The metal-insulator transition in Fe_{1.01-x}Cu_xSe, *Journal of Physics: Condensed Matter* **21**, 305701 (2009).
- [16] S. Huh, Z. Lu, Y. S. Kim, D. Kim, S. Liu, M. Ma, L. Yu, F. Zhou, X. Dong, C. Kim, and Z. Zhao, Cu doping effects on the electronic structure of Fe_{1-x}Cu_xSe, *2110.14463* (2021).
- [17] B.-L. Young, J. Wu, T.-W. Huang, K.-W. Yeh, and M.-K. Wu, Magnetic fluctuations in FeSe_{1-δ} and Cu-doped FeSe_{1-δ}: ⁷⁷Se NMR experiments, *Phys. Rev. B* **81**, 144513 (2010).
- [18] L. M. Schoop, S. A. Medvedev, V. Ksenofontov, A. Williams, T. Palasyuk, I. A. Troyan, J. Schmitt, F. Casper, C. Wang, M. Erements, R. J. Cava, and C. Felser, Pressure-restored superconductivity in Cu-substituted FeSe, *Phys. Rev. B* **84**, 174505 (2011).
- [19] L. Deng, T. Bontke, R. Dahal, Y. Xie, B. Gao, X. Li, K. Yin, M. Gooch, D. Rolston, T. Chen, Z. Wu, Y. Ma, P. Dai, and C.-W. Chu, Pressure-induced high-temperature superconductivity retained without pressure in FeSe single crystals, *Proceedings of the National Academy of Sciences* **118**, 10.1073/pnas.2108938118 (2021).
- [20] M. N. Gastiasoro and B. M. Andersen, Enhancing superconductivity by disorder, *Phys. Rev. B* **98**, 184510 (2018).
- [21] D. Chareev, E. Osadchii, T. Kuzmicheva, J.-Y. Lin, S. Kuzmichev, O. Volkova, and A. Vasiliev, Single crystal growth and characterization of tetragonal FeSe_{1-x} superconductors, *CrystEngComm* **15**, 1989 (2013).
- [22] A. E. Böhmer, V. Taufour, W. E. Straszheim, T. Wolf, and P. C. Canfield, Variation of transition temperatures and residual resistivity ratio in vapor-grown FeSe, *Phys. Rev. B* **94**, 024526 (2016).
- [23] A. Eiling and J. S. Schilling, Pressure and temperature dependence of electrical resistivity of Pb and Sn from 1-300K and 0-10 GPa-use as continuous resistive pressure monitor accurate over wide temperature range. superconductivity under pressure in Pb, Sn and In, *Journal of Physics F: Metal Physics* **11**, 623 (1981).
- [24] G.-Y. Chen, E. Wang, X. Zhu, and H.-H. Wen, Synergy and competition between superconductivity and antiferromagnetism in FeSe under pressure, *Phys. Rev. B* **99**, 054517 (2019).
- [25] See supplemental material for further experimental data and analysis complementary to the main manuscript.
- [26] E. Gati, A. E. Böhmer, S. L. Bud'ko, and P. C. Canfield, Bulk Superconductivity and Role of Fluctuations in the Iron-Based Superconductor FeSe at High Pressures, *Phys. Rev. Lett.* **123**, 167002 (2019).
- [27] M. Bristow, P. Reiss, A. A. Haghighirad, Z. Zajicek, S. J. Singh, T. Wolf, D. Graf, W. Knafo, A. McCollam, and A. I. Coldea,

- Anomalous high-magnetic field electronic state of the nematic superconductors $\text{FeSe}_{1-x}\text{S}_x$, *Phys. Rev. Research* **2**, 013309 (2020).
- [28] P. Reiss, D. Graf, A. A. Haghighirad, W. Knafo, L. Drigo, M. Bristow, A. Schofield, and A. I. Coldea, Quenched nematic criticality and two superconducting domes in an iron-based superconductor, *Nature Physics* **16**, 89 (2020).
- [29] T. Terashima, N. Kikugawa, S. Kasahara, T. Watashige, T. Shibauchi, Y. Matsuda, T. Wolf, A. E. Böhrer, F. Hardy, C. Meingast, H. v. Löhneysen, and S. Uji, Pressure-Induced Antiferromagnetic Transition and Phase Diagram in FeSe, *J. Phys. Soc. Japan* **84**, 063701 (2015).
- [30] L. Xiang, U. S. Kaluarachchi, A. E. Böhrer, V. Taufour, M. A. Tanatar, R. Prozorov, S. L. Bud'ko, and P. C. Canfield, Dome of magnetic order inside the nematic phase of sulfur-substituted FeSe under pressure, *Phys. Rev. B* **96**, 024511 (2017).
- [31] K. Rana, L. Xiang, P. Wiecek, R. A. Ribeiro, G. G. Lesseux, A. E. Böhrer, S. L. Bud'ko, P. C. Canfield, and Y. Furukawa, Impact of nematicity on the relationship between antiferromagnetic fluctuations and superconductivity in $\text{FeSe}_{0.91}\text{S}_{0.09}$ under pressure, *Phys. Rev. B* **101**, 180503 (2020).
- [32] P. S. Wang, S. S. Sun, Y. Cui, W. H. Song, T. R. Li, R. Yu, H. Lei, and W. Yu, Pressure Induced Stripe-Order Antiferromagnetism and First-Order Phase Transition in FeSe, *Phys. Rev. Lett.* **117**, 237001 (2016).
- [33] M. D. Watson, T. Yamashita, S. Kasahara, W. Knafo, M. Nardone, J. Béard, F. Hardy, A. McCollam, A. Narayanan, S. F. Blake, T. Wolf, A. A. Haghighirad, C. Meingast, A. J. Schofield, H. v. Löhneysen, Y. Matsuda, A. I. Coldea, and T. Shibauchi, Dichotomy between the Hole and Electron Behavior in Multiband Superconductor FeSe Probed by Ultrahigh Magnetic Fields, *Phys. Rev. Lett.* **115**, 027006 (2015).
- [34] L. S. Farrar, M. Bristow, O. Humphries, Z. Zajicek, A. A. Haghighirad, A. McCollam, S. J. Bending, and A. I. Coldea, Unconventional localization of electrons inside of a nematic electronic phase, submitted (2022).
- [35] J. P. Sun, G. Z. Ye, P. Shahi, J.-Q. Yan, K. Matsuura, H. Kontani, G. M. Zhang, Q. Zhou, B. C. Sales, T. Shibauchi, Y. Uwatoko, D. J. Singh, and J.-G. Cheng, High- T_c Superconductivity in FeSe at High Pressure: Dominant Hole Carriers and Enhanced Spin Fluctuations, *Phys. Rev. Lett.* **118**, 147004 (2017).
- [36] M. D. Watson, T. K. Kim, A. A. Haghighirad, S. F. Blake, N. R. Davies, M. Hoesch, T. Wolf, and A. I. Coldea, Suppression of orbital ordering by chemical pressure in $\text{FeSe}_{1-x}\text{S}_x$, *Phys. Rev. B* **92**, 121108 (2015).
- [37] T. Terashima, N. Kikugawa, S. Kasahara, T. Watashige, Y. Matsuda, T. Shibauchi, and S. Uji, Magnetotransport study of the pressure-induced antiferromagnetic phase in FeSe, *Phys. Rev. B* **93**, 180503 (2016).
- [38] H. Okabe, N. Takeshita, K. Horigane, T. Muranaka, and J. Akimitsu, Pressure-induced high- T_c superconducting phase in fese: Correlation between anion height and T_c , *Phys. Rev. B* **81**, 205119 (2010).
- [39] K. Miyoshi, K. Morishita, E. Mutou, M. Kondo, O. Seida, K. Fujiwara, J. Takeuchi, and S. Nishigori, Enhanced superconductivity on the tetragonal lattice in fese under hydrostatic pressure, *Journal of the Physical Society of Japan* **83**, 013702 (2014).
- [40] J. Xie, X. Liu, W. Zhang, S. M. Wong, X. Zhou, Y. Zhao, S. Wang, K. T. Lai, and S. K. Goh, Fragile Pressure-Induced Magnetism in FeSe Superconductors with a Thickness Reduction, *Nano Letters* **21**, 9310 (2021), pMID: 34714653, <https://doi.org/10.1021/acs.nanolett.1c03508>.
- [41] M. M. Korshunov, Y. N. Togushova, and O. V. Dolgov, Impurities in multiband superconductors, *Physics-Uspekhi* **59**, 1211 (2016).
- [42] D. V. Efremov, M. M. Korshunov, O. V. Dolgov, A. A. Golubov, and P. J. Hirschfeld, Disorder-induced transition between s_{\pm} and s_{++} states in two-band superconductors, *Phys. Rev. B* **84**, 180512 (2011).
- [43] B. M. Andersen, S. Graser, and P. J. Hirschfeld, Disorder-Induced Freezing of Dynamical Spin Fluctuations in Underdoped Cuprate Superconductors, *Phys. Rev. Lett.* **105**, 147002 (2010).
- [44] M. Bendele, A. Ichsanow, Y. Pashkevich, L. Keller, T. Strässle, A. Gusev, E. Pomjakushina, K. Conder, R. Khasanov, and H. Keller, Coexistence of superconductivity and magnetism in FeSe_{1-x} under pressure, *Phys. Rev. B* **85**, 064517 (2012).
- [45] J. H. J. Martiny, A. Kreisel, and B. M. Andersen, Theoretical study of impurity-induced magnetism in FeSe, *Phys. Rev. B* **99**, 014509 (2019).
- [46] M. N. Gastiasoro, P. J. Hirschfeld, and B. M. Andersen, Origin of electronic dimers in the spin-density wave phase of Fe-based superconductors, *Phys. Rev. B* **89**, 100502 (2014).
- [47] D. F. Mross and T. Senthil, Spin- and pair-density-wave glasses, *Phys. Rev. X* **5**, 031008 (2015).
- [48] O. Humphries, A. A. Haghighirad, M. Bruma, T. Wolf, and A. I. Coldea, The complex mobility spectrum of the multi-band nematic superconductors, $\text{FeSe}_{1-x}\text{S}_x$, in preparation (2022).

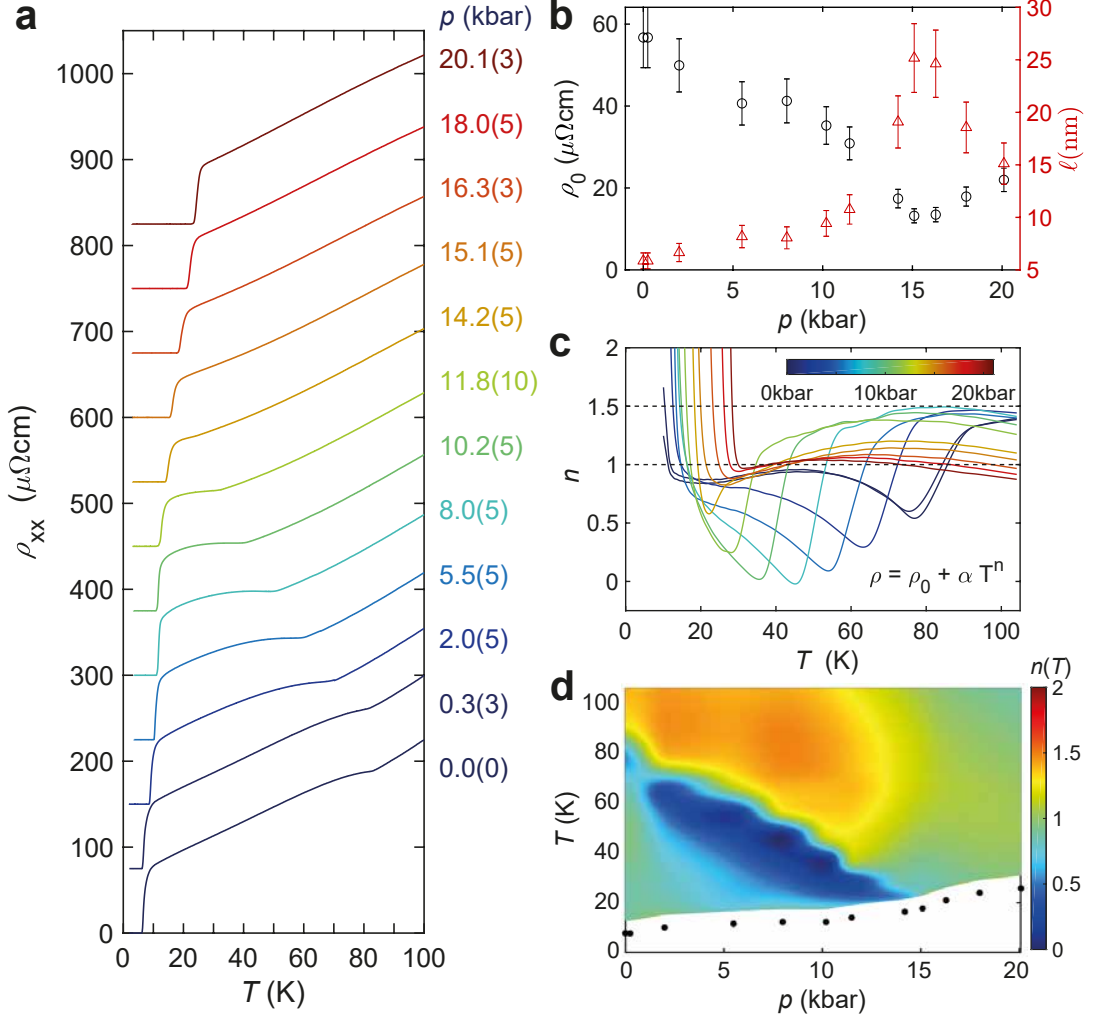


FIG. S1. **The zero-field resistivity and the local resistivity exponent.** (a) Temperature dependence of the resistivity as a function of applied pressure. The curves are shifted for clarity (by $75\mu\Omega\text{cm}$ each). The pressure of each run is given by the corresponding colour. The non-shifted curves are shown in Fig. 1(a). The resistivity can be expressed using the form $\rho = \rho_0 + \alpha T^n$, where n is the local resistivity temperature exponent. At ambient pressure the zero-temperature resistivity, ρ_0 , is obtained by using high magnetic fields to suppress the superconductivity at temperatures below T_c and extrapolating the high-field dependence at zero-field for each temperature [14]. The mean free path, $\ell = \frac{\pi c h}{N e^2 k_F \rho_0}$, is calculated using the ambient pressure values for c and k_F [14]. (b) The pressure dependence of the zero-temperature resistivity, ρ_0 , extracted from a linear extrapolation of the zero-field resistivity above the onset of superconductivity similar to the ambient pressure dependence [14]. The red triangles are the mean free path, using the ρ_0 values. (c) The temperature dependence of the local resistivity exponent, n , for different pressures in zero magnetic field and (d) its interpolated colour map for different pressures.

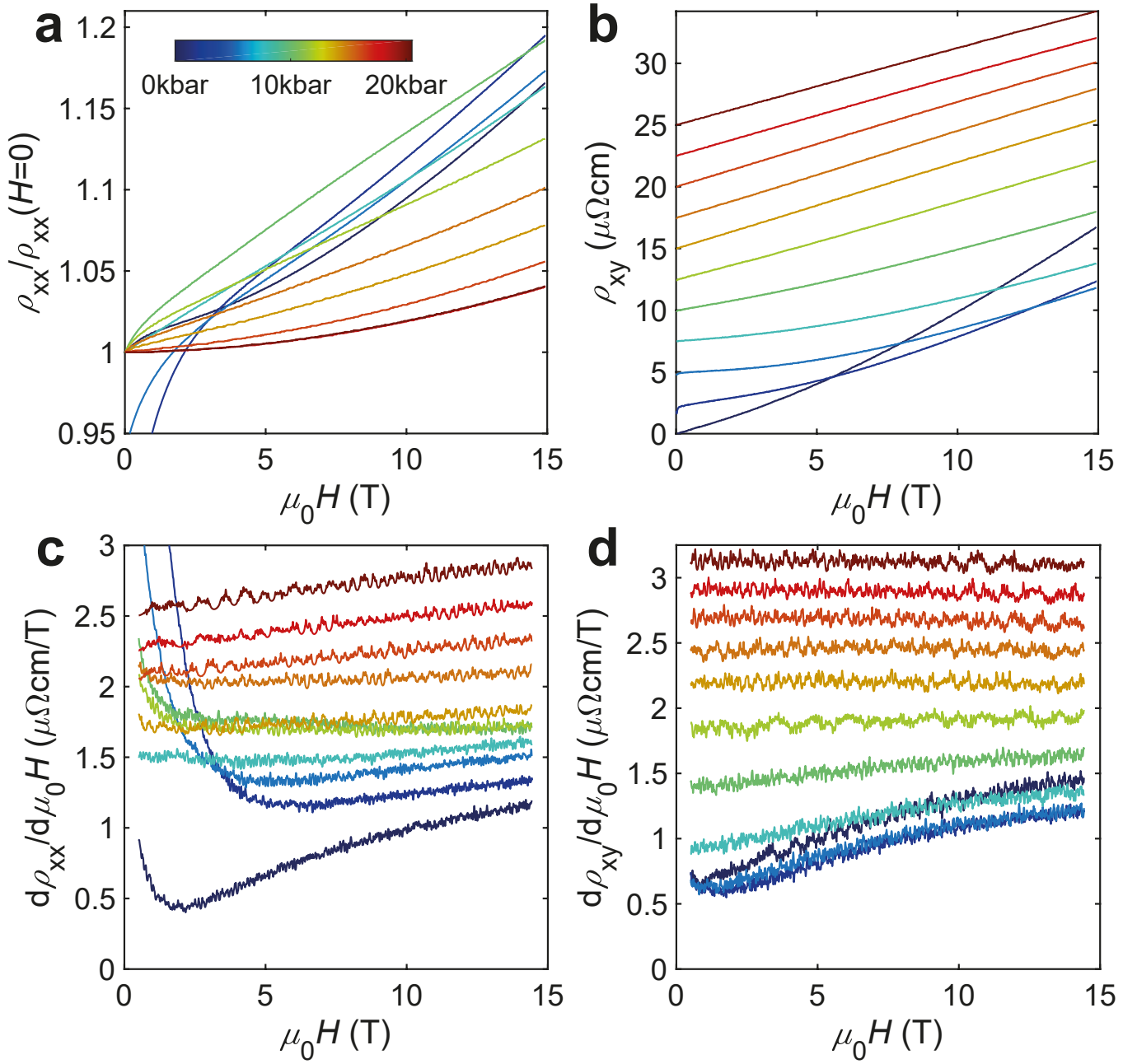


FIG. S2. **Magnetotransport behaviour in the normal phase.** The field dependence of (a) ρ_{xx} and (b) ρ_{xy} at a fixed temperature close to the onset of superconductivity for different pressures and their corresponding derivatives in relation to the magnetic field in (c) and (d), respectively. The derivatives in magnetic field of the ρ_{xy} component shows a constant behaviour at high-pressures above 10 kbar indicative of a two-band behaviour.

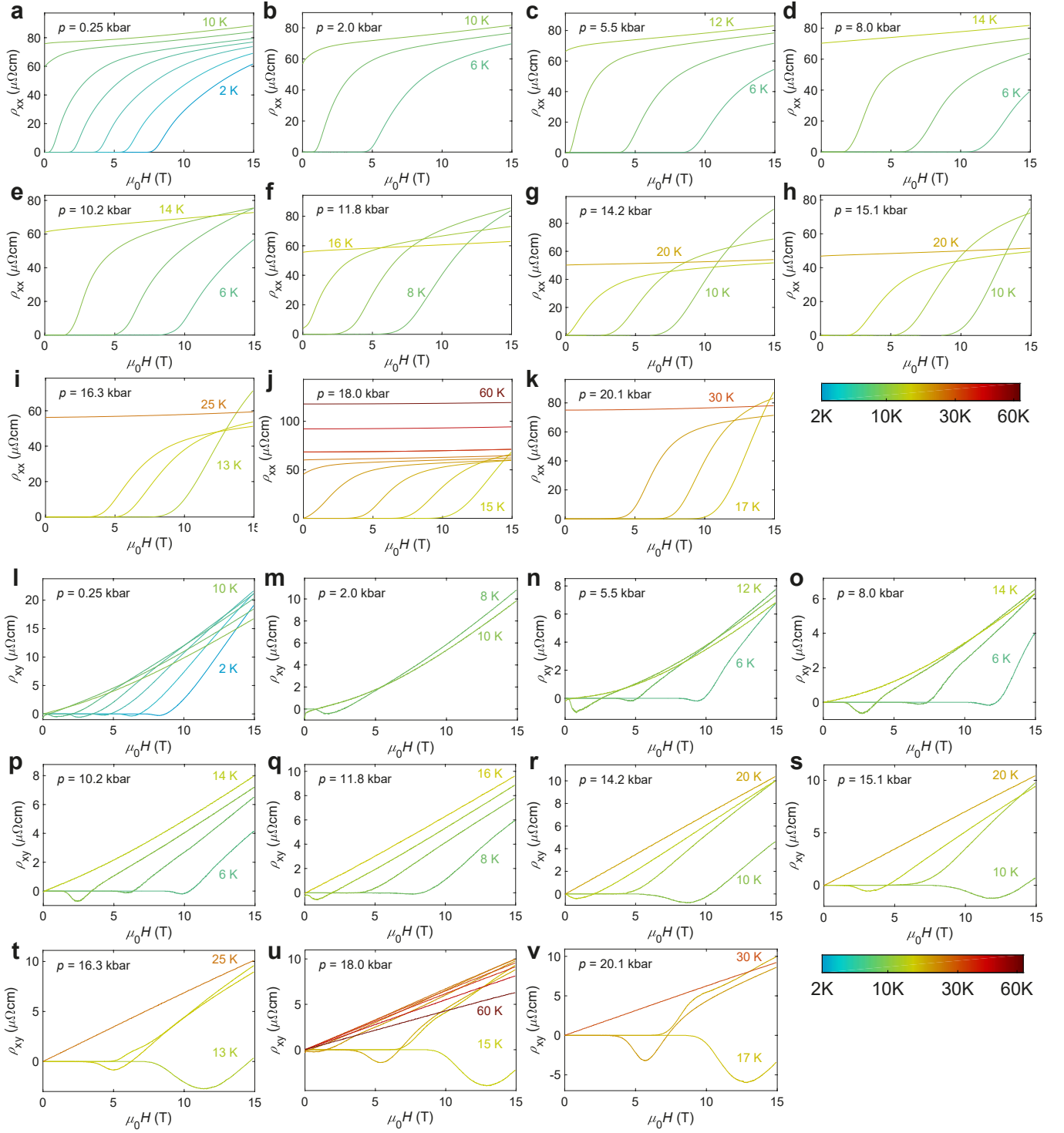


FIG. S3. **Magnetotransport behaviour at different pressures.** The field-dependence of (a) ρ_{xx} and (b) ρ_{xy} measured at different constant temperatures. Each panel corresponds to different applied pressure.

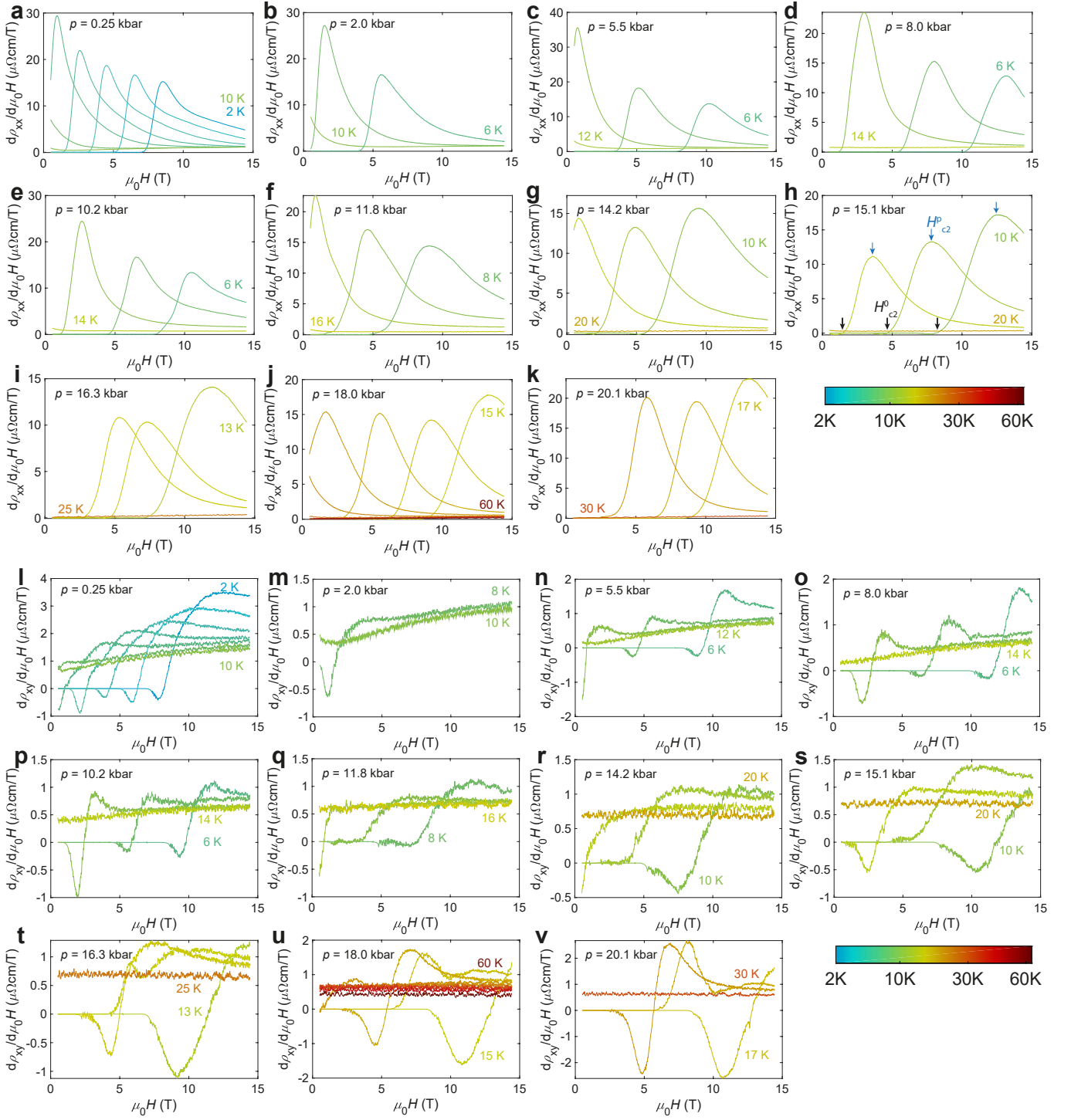


FIG. S4. **The derivative of magnetotransport curves in relation to magnetic field at different pressures.** Derivatives with respect to magnetic field for (a) ρ_{xx} and (b) ρ_{xy} as a function of magnetic field measured at different constant temperatures. Each panel corresponds to different applied pressures. Examples of how the critical field was extracted are shown in (h). The peak of the derivative is referred to as H_{c2}^p , and the zero extrapolation as H_{c2}^0 .

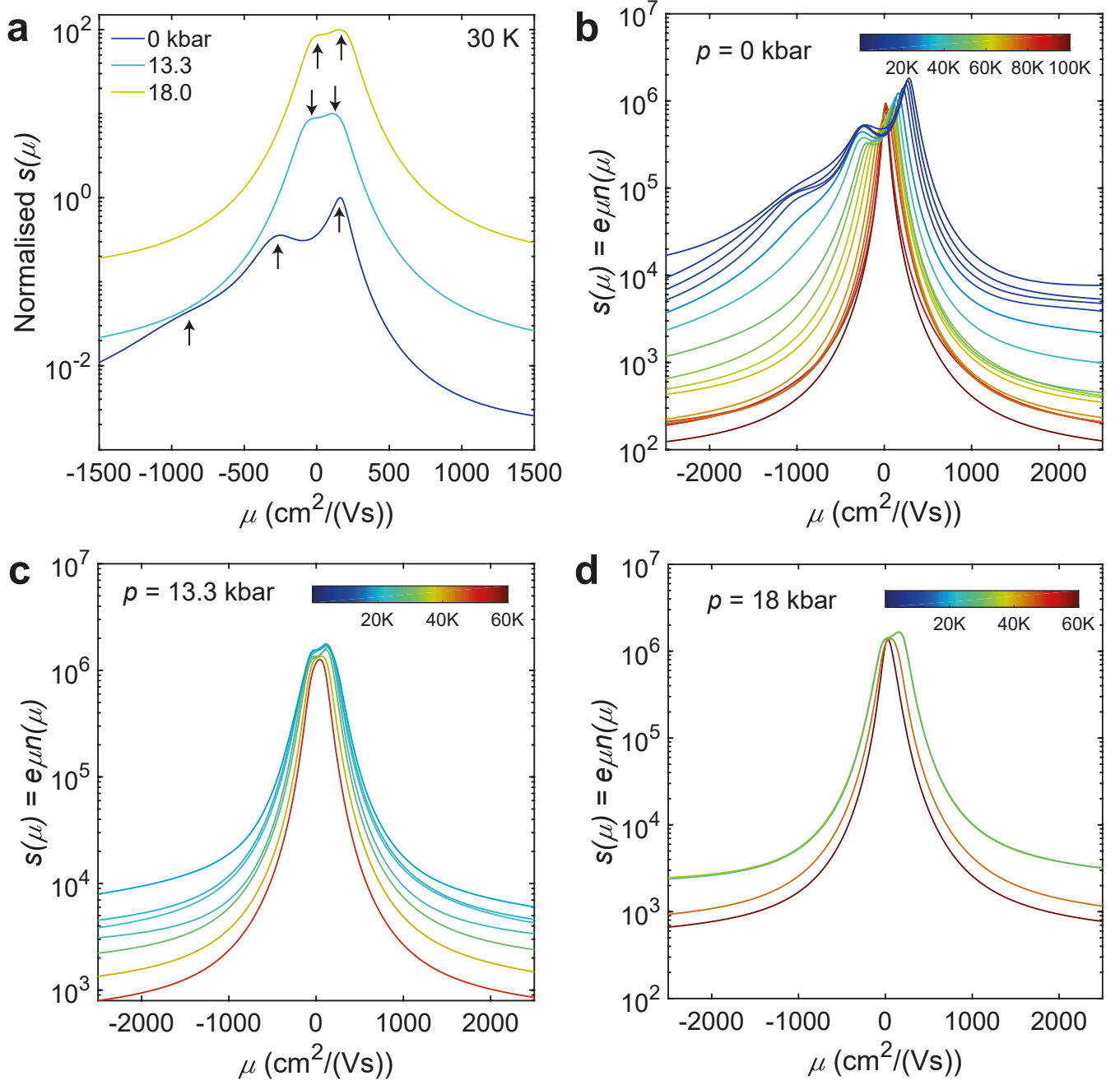


FIG. S5. **Mobility spectrum at different pressures.** (a) The mobility spectrum extracted from magnetotransport data [48] for different pressures at 30 K. Arrows indicated the positions of mobilities for the positive and negative charge carriers. Mobility spectrum extracted for constant temperatures at different pressures of (b) 0 kbar, (c) 13.3 kbar and (d) 18 kbar, respectively.

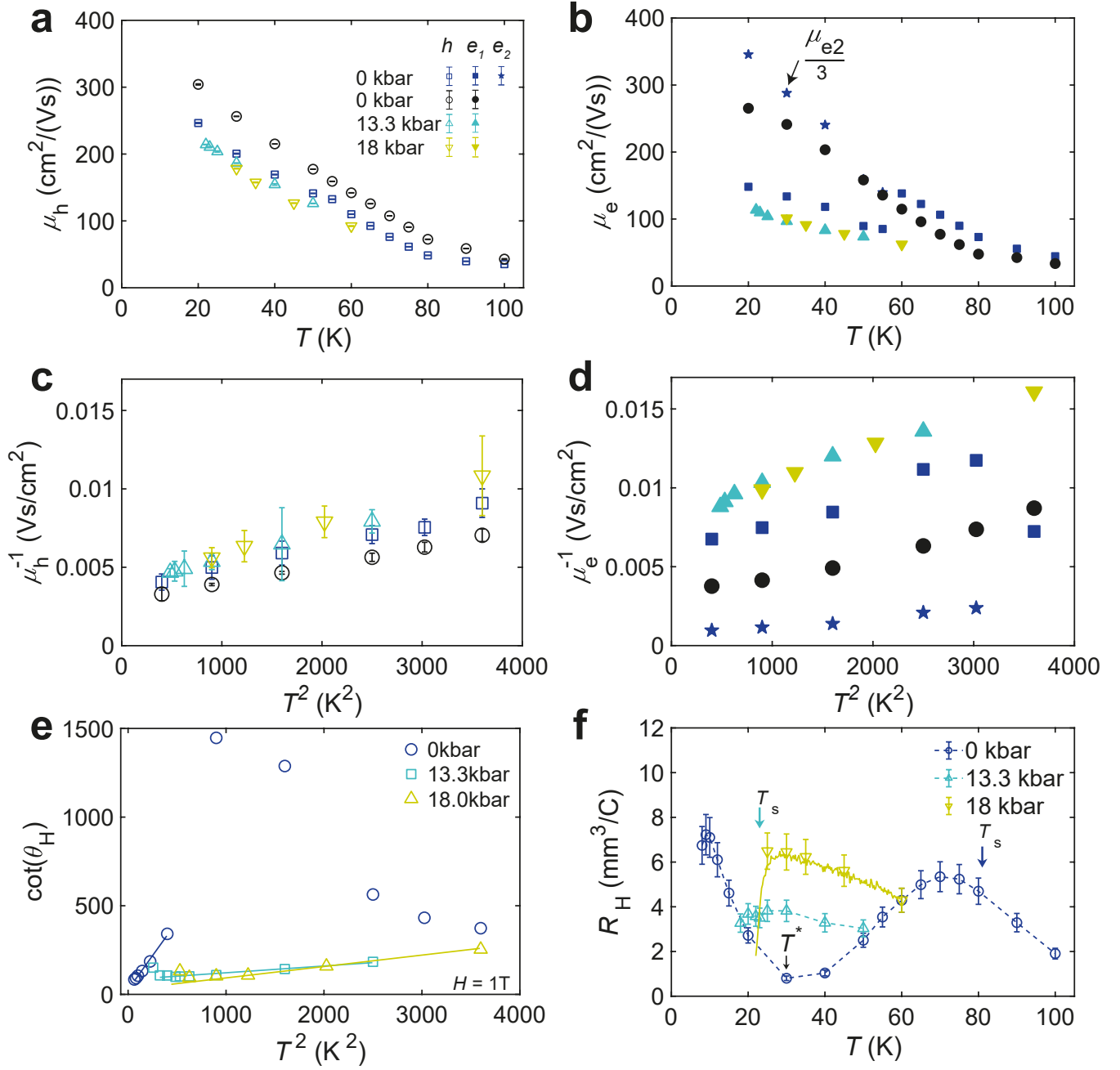


FIG. S6. **Mobility spectrum at different pressures.** The mobility temperature dependence for (a) positive charge carriers (holes) and (b) the negative charge carriers (electrons). The ambient pressure data is modelled using a three-band model, described in the Ref. 14, whilst the two-band model is taken from low-field limit (< 7 T) only. The mobility of the second electron carrier, e_2 , in (b) is scaled by a factor $1/3$. The inverse mobility against a T^2 dependence for (c) holes and (d) electrons. (e) $\cot(\theta_H)$, cotangent of the Hall angle defined, temperature dependence. Solid lines are fit to linear regions at higher temperatures. The values are taken from field-dependent measurements and chosen at a fixed field value for all temperatures. (f) The Hall coefficient, R_H , temperature dependence for different pressures of Cu-FeSe. The dashed lines are guide to the eye. The solid line for 13.3 kbar is from a temperature sweep measured in constant field of 1 T. T^* marks the minimum in R_H for 0 kbar.